HHS Public Access

Author manuscript

Pharm Res. Author manuscript; available in PMC 2024 February 20.

Published in final edited form as:

Pharm Res. 2023 September ; 40(9): 2121–2131. doi:10.1007/s11095-023-03593-y.

TIMP-1 Protects Tight Junctions of Brain Endothelial Cells From MMP-Mediated Degradation

Hannaneh Ahmadighadykolaei[1], **Janet A. Lambert**[1,2], **Maryam Raeeszadeh-Sarmazdeh**[1]

[1]Department of Chemical and Materials Engineering, University of Nevada, 1664 N. Virginia St, Reno, NV 89557, USA

[2]Department of Pharmacology, University of Nevada, Reno School of Medicine, Reno, NV, USA

Abstract

Objective—The blood–brain barrier (BBB) plays a critical role in central nervous system homeostasis, and the integrity of BBB is disrupted in many neurodegenerative diseases. Matrix metalloproteinases (MMPs) degrade the tight junctions (TJs) of endothelial cells and basement membrane components essential to BBB integrity, which leads to increased BBB permeability and allows inflammatory cells and neurotoxic substances to enter the brain. Tissue inhibitors of metalloproteinases (TIMPs), endogenous inhibitors of MMPs, regulate MMP activity, thereby maintaining BBB integrity.

Methods—The disruptive impacts of MMP-3 and MMP-9 on BBB and protective effect of TIMP-1 were investigated in a simplified *in vitro* model of the BBB, which was generated using rat brain microvascular endothelial cells (RBMEC). The main features of BBB formation, including permeability and the trans-endothelial electrical resistance (TEER), were monitored over time after the addition of MMP-3 and MMP-9 and their complexes with TIMP-1 inhibitor.

Results—Our results indicated that MMP-3 and MMP-9 caused a dose-dependent disruption of the BBB, with 1.5 μM MMPs resulting in an over threefold increase in permeability, while TIMP-1 inhibition protected the integrity of the BBB model and recovered TEER and permeability of RBMECs. The disruption and recovery of tight junction proteins of RBMECs after MMP and TIMP treatment were also detected using fluorescent microscopy.

Conclusion—MMP-9 and MMP-3 disrupt the BBB by degrading tight junctions in endothelial cells, and TIMP-1 could inhibit the disruptive effect of MMP-3 and MMP-9 by showing potential as therapeutic protein against MMP-related diseases where BBB disruption plays a role.

Keywords

blood-brain barrier (BBB); drug delivery; matrix metalloproteinases (MMPs); neurodegenerative diseases; tissue Inhibitors of metalloproteinases (TIMPs)

Maryam Raeeszadeh-Sarmazdeh, maryamr@unr.edu.

Author contributions M. R.-S., conception; H. A. and J. A. L., performing the experiments; H. A, J. A. L., M. R.-S., data analysis, writing and editing the manuscript drafts. M. R.-S. funding and supervision.

Supplementary Information The online version contains supplementary material available at https://doi.org/10.1007/s11095-023-03593-y.

Conflict of interest The authors have no conflict of interest.

Introduction

Enzymes of the matrix metalloproteinase (MMP) family are proteases responsible for the remodeling of the extra-cellular matrix (ECM). Additionally, they contribute to the disruption of the BBB [1-3] by degrading tight junctions (TJs) between endothelial cells. MMPs can also cause BBB disruption by targeting proteins in the basal lamina, such as laminin, heparan sulfate proteoglycans, and fibronectin [4-8]. MMPs play a role in the common pathways involved in the neuroinflammatory response in many neurological disorders. In neuroinflammatory conditions, such as Alzheimer's disease, Parkinson's disease, multiple sclerosis, and traumatic brain injury, MMPs are activated in response to inflammation. They break down components of the ECM, including those that maintain the integrity of the BBB [4, 5]. This leads to increased permeability of the BBB and allows inflammatory cells and neurotoxic substances to enter the brain, exacerbating neuroinflammation and neurodegeneration [9]. The regulation of the permeability and systemic filtration of the BBB is controlled by TJ protein complexes by sealing the intercellular space between adjacent brain microvascular endothelial cells [10-12].

Among MMPs, studies have indicated that MMP-3 and MMP-9 are involved directly in disruption of BBB. Initial *in vivo* evidence suggests that MMP-3 targets basal lamina and TJ proteins, which results in BBB disruption and allows neutrophils to penetrate the brain. Independent of other factors, pericytes and microglia release MMP-3, leading to cerebral blood vessel injury [9]. MMP-3 is also co-localized to human cerebral endothelial cells (HCEC) and is involved in the processing of other MMPs [13, 14]. MMP-3 is known to target numerous proteins within the ECM and can activate MMP-9 *in vitro*. As a result, MMP-3 plays a role in the proteolytic breakdown of the BBB by targeting key components of the basal lamina and TJs [9]. MMP-9 is associated with BBB disruption and increased permeability in conditions such as stroke, traumatic brain injury, and multiple sclerosis [1, 15]. MMP-9 can cleave TJ proteins and ECM components that are crucial for maintaining BBB integrity [16, 17]. In addition to its effects on the BBB, MMP-9 has been shown to directly contribute to neuronal damage by cleaving synaptic proteins and promoting neuroinflammatory signaling pathways. MMP-9 is thus considered a promising target for therapeutic intervention in neurological disorders, and there is interest in developing drugs that can selectively inhibit MMP-9 activity and protect against BBB disruption and neurodegeneration.

MMPs are expressed as zymogens and their activity can be modulated through the formation of complexes with naturally occurring endogenous inhibitor proteins, tissue inhibitors of metalloproteinases (TIMPs) [18-23]. When metalloproteinase activity is dysregulated, it results in uncontrolled degradation of the ECM, disruption of intercellular junctions, and the propagation of a proinflammatory microenvironment, which are all linked to several pathologies. TIMPs are essential regulators of ECM turnover, intercellular junction stability, and endothelial signaling [24, 25]. TIMP-1 is a known inhibitor of both MMP-3 and MMP-9 with pM affinity inhibition [26], making it a great candidate to protect MMP-mediated BBB disruption. Treatment with TIMP-1 attenuated BBB disruption and improved neurological outcomes in a mouse model of intracerebral hemorrhage [27]. The protective effect of

TIMP-1 was attributed to the inhibition of MMP-9, which is known to contribute to BBB disruption and cerebral edema in ischemic stroke [28]. Overall, the available evidence suggests that TIMP-1 can protect the BBB by inhibiting the activity of MMP-3 and MMP-9, thereby preventing the degradation of endothelial cell tight junctions that are critical in maintaining the integrity of the BBB.

In this study, an *in vitro* model of the BBB was made using rat brain microvascular endothelial cells (RBMEC), with a trans-endothelial electrical resistance (TEER) of more than 150 $\Omega \cdot cm^2$. The disruption and protection of BBB was then analyzed by permeability, TEER, and immunocytochemistry (ICC) after treating with MMP-3, and MMP-9 or their protein complexes with TIMP-1.

TEER and permeability analysis are important measures of the integrity of the BBB. TEER measures the resistance of electrical current across endothelial cells that form the lining of blood vessels, which correlates with the tightness of the cell junctions critical for maintaining selective permeability [29-34]. High TEER values indicate strong tight junctions and low permeability, while low TEER values indicate weak tight junctions and high permeability. Permeability measures the ability of substances to cross the BBB. Changes in BBB permeability can occur due to injury, inflammation, or disease. Both TEER and permeability measurements are used to evaluate BBB integrity, and changes in either of these parameters can indicate disruption or dysfunction of the BBB. ICC also can be a useful tool for investigating the expression and distribution of BBB-related proteins, such as TJ proteins.

Methods

Protein expression, purification

The catalytic domains of MMP-3 (MMP-3 cd) and MMP-9 (MMP-9 cd), were expressed as recombinant proteins in Rosetta™ (DE3) pLysS cells (Sigma Aldrich, MO, USA) and resolubilized from the inclusion bodies and purified using either affinity chromatography or anionic exchange as previously described [35, 36]. Recombinant full-length TIMP-1 protein was expressed in human FreeStyle™ 293-F cells (ThermoFisher Scientific, Waltham, MA, USA), and purified by ion exchange and size-exclusion chromatography as previously reported. To measure TIMP-1 protein concentration, titration against MMP-3 cd protein stock of known concentration was used [37, 38].

RBMEC culture

RBMEC isolated from adult CD® IGS rat brains were obtained from ScienCell (Carlsbad, CA, USA). RBMEC cultures were maintained at 37°C in a humidified atmosphere with 5% CO_2 on fibronectin-coated culture vessels (2 $\mu g/cm^2$) according to manufacturer's recommendations in endothelial cell media (ScienCell #1021). RBMEC were passaged up to three times when the cultures reached 80%-90% confluency, with brief treatment with 0.25% Trypsin/EDTA (ThermoFisher Scientific, Waltham, MA, USA) to passage cells.

Establishment of *in vitro* BBB model

RBMECs (50,000 cells/cm^2) were seeded on the upper side of 0.4 μm pore size 12- or 24-well (with surface areas of 1.12 cm^2 or 0.33 cm^2, respectively) Corning Transwell® polyester inserts (Corning, NY, USA) coated with 0.4 mg/mL type IV collagen (Sigma-Aldrich, CA, USA) and 0.1 mg/mL fibronectin (Sigma-Aldrich, CA, USA) in Dulbecco's phosphate buffered saline (DPBS, ThermoFisher Scientific, Waltham, MA, USA) for at least 4 h prior to adding cells. Transwells containing cells and either 100 μL (24 well) or 500 μL (12 well) endothelial cell media were then placed in the wells of the companion plates containing 600 μL (24 well) or 1500 μL (12 well) media (Fig. 1) and incubated at 37°C and 5% CO_2 until cells reached confluence, whereupon the media was changed to serum free endothelial cell media (sfECM) supplemented with 0.55 nM hydrocortisone and the cells incubated overnight.

Permeability assays

The sfECM in both Transwell® chambers was changed at least 1 h prior to addition of proteins. MMP-3 cd, MMP-9 cd, TIMP-1 were mixed and incubated at 37°C for 1 h before adding proteins to sfECM containing 10 kDa fluorescein isothiocyanate (FITC) dextran (1 μM final, Sigma, St. Louis, MO, USA). At t = 0, the protein/FITC-dextran mixtures were added to apical chambers and 60 μL (24 well) or 150 μL (12 well) samples (i.e., 10% of the volume of the basolateral chamber) were taken with replacement from the basolateral chamber at 15 to 30 min intervals for 120 to 150 min. Fluorescence was measured using a Synergy microplate reader with excitation at 485/20 and emission at 528/20 and a gain of 84.

Background fluorescence from FITC-dextran free sfECM medium was subtracted from each sample. The signal was corrected for sampling due to the replacement of the removed volume for each timepoint after the first by multiplying the background subtracted reading by 1.1. The clearance volume ($V_{C,t}$) at each time point was calculated by dividing the corrected reading by S_a, the reading in its apical chamber, and multiplying by the volume of media in the Transwell's basolateral chamber (600 μL in 24 well or 1500 μL in 12 well). Linear regression in GraphPad Prism 9 was used to calculate the slope m of clearance volume *versus* time. Permeability (Pe) was calculated by subtracting the reciprocal of the slope of the blank (no cells) from the reciprocal of the slope of each sample. Pe's % error was calculated by dividing the standard error of the slope by the slope then the % error was multiplied by the Pe. The p value was calculated by GraphPad Prism 9 through ordinary one-way ANOVA.

TEER measurements

After one day after changing the media on Transwell® to serum-free media, the TEER was measured with an EVOM3 resistance meter (World Precision Instruments, Sarasota, FL, USA) by placing one electrode inside the Transwell apical chamber and the other outside in the well following the manufacture protocol; then the media removed from both Transwell® chambers and replaced with pre-warmed fresh media and returned to incubator for 60 min. TEER was rechecked to verify that the TEER had recovered to more than 150 Ω × cm^2, then

the endothelial monolayers were treated with MMPs and TIMPs that already incubated for 1 h and then the TEER was measured at 30 min intervals for 2 h.

The resistance measurements of collagen/fibronectin-coated Transwells without cells (blank) were subtracted from those with cells to determine the final TEER value, which was calculated using the formula: TEER = (sample TEER value – background TEER value) × area of the insert membrane. The results are reported in units of $\Omega \times cm^2$ and reflect the change in TEER relative to the control.

ICC of RBMEC

To verify the presence of TJs, 50,000 RBMEC were plated on 35 mm glass base dishes (Thermo Scientific, Rochester, NY, USA) coated with 2 $\mu g/cm^2$ fibronectin. After reaching 90% confluency, the cells were treated or not 1.5 μM MMP-3 cd and/or 1.5 μM TIMP-1 for 1 h before washing once with DPBS and fixation with 4% paraformaldehyde for 15 min at room temperature. Cells were permeabilized with 0.1% Triton X-100 (Sigma-Aldrich, CA, USA) and blocked with 5% bovine serum albumin (BSA) in DPBS. To perform immunofluorescent staining of TJ proteins, the cells were incubated overnight at 4°C with a 1/50 dilution of polyclonal rabbit antibody against ZO-1 (ThermoFisher Scientific, Waltham, MA, USA, cat # 40–2200) in 1% BSA. After washing in 3 times DPBS, a 1/1000 dilution of an Alexa Fluor 488-conjugated secondary anti-rabbit antibody (Invitrogen, Life Technologies) in 1% BSA in DPBS was applied for one hour at room temperature. Cells were imaged using a confocal laser-scanning microscope at 60X magnification (FV1000 microscope, Olympus Corporation, Shinjuku City, Tokyo, Japan). The images were analyzed by using FV10-ASW 4.2 Viewer software.

Results

RBMEC exhibit indicators of BBB formation

Several previous studies have used RBMEC as an *in vitro* model to study the BBB, although it lacks other important cell types present in the BBB *in vivo*, such as pericytes and astrocytes [32, 39, 40]. TEER was measured using an EVOM3 meter and represents resistance formed between the cells grown in the apical chamber of a Transwell insert and the media in the well, which is an indicator of TJ formation in RBMEC cells. TEER values were increased from 17 $\Omega \cdot cm^2$ right after plating RBMEC (time 0) to 150 $\Omega \cdot cm^2$ after 24 h (Fig. 2a) consistent with previous *in vitro* BBB studies [41-43]. The RBMEC cells grown to confluency on Transwells after 24 h were shown using an inverted bright field microscope where the blank represents the collagen/fibronectin-coated Transwell only with no cells grown on it. After confluency was reached, cells were transferred to sfECM supplemented with 0.55 nM hydrocortisone overnight and experiments were performed when TEER exceeded 150 $\Omega \cdot cm^2$.

Permeability of the RBMECs were measured by the rates of diffusion of FITC-dextran (MW = 10 kDa) between RBMEC that form TJs were compared with 3T3 cells that do not, with or without treatment of recombinant purified MMP-3 cd protein by taking samples from the well and reading the fluorescent level using a microplate reader (Fig. 1). TJ

formation results in a decrease in the permeability of FITC-dextran as it diffuses from the apical to the basolateral chamber, but MMP-3-mediated disruption of TJs increases the rate of permeability [32]. Our results indicated that dextran diffused the most rapidly through blank (collagen/fibronectin-coated Transwell, no cells), then 3T3 cells, and slowest through RBMEC (Fig. 3a) which suggests TJ formation in RBMEC. The permeability of control 3T3 cells was approximately 2.5-fold higher than RBMEC (Fig. 3b). The TEER values for RBMECs were more than 150 $\Omega \times cm^2$ compared to less than 10 $\Omega \times cm^2$ for the 3T3 cells (Fig. 3c) further indicating increased resistance resulting from TJ formation. FITC-dextran molecules diffused more rapidly through RBMEC treated with MMP-3 cd protein in a dose-dependent manner (Fig. 4b), leading to a 2.26-fold increase over baseline permeability at 0.5 μM of MMP-3 cd (Fig. 4b); while, in the case of 3T3, addition of MMP-3 cd did not result in any observable change in permeability (Fig. 4a). The decrease in permeability and increase in TEER values in RBMEC indicate TJ formation, which is characteristic of the intact BBB.

Effects of MMPs and TIMPs on permeability of the *in vitro* BBB model

The effect of MMP-mediated degradation of TJ and the MMP inhibitory effect of TIMPs on TJ integrity was studied by measuring the rate of FITC-dextran diffusion (permeability assay) and TEER over time after the RBMECs on Transwells were treated with different concentrations of MMP-3 cd, MMP-9 cd and/or a complex of TIMP-1 with MMP-3 cd or MMP-9 cd. All experiments were performed when the RBMEC reached to 90% confluency confirmed by microscopy of RBMEC on 24 insert wells. After 24 h of RBMEC growth, the average TEER value of 17 different RBMECs on Transwell inserts was shown to be more than 150 $\Omega \times cm^2$ (Fig. 2). Each culture condition was replicated independently five times. Treatment of RBMECs with MMP-3 cd protein showed a dose-dependent increase in permeability similar to previous studies [27, 44] suggesting MMP-3 cd disrupted the TJs between RBMECs, which resulted in a nearly 18-fold increase over baseline permeability at 1.5 μM of MMP-3 cd (Fig. 5a). TIMP-1, an endogenous inhibitor of MMP-3 and MMP-9 with pM affinity [26, 45], was used to inhibit MMP-mediated disruption of TJs in RBMECs. In the presence of 1.5 μM of TIMP-1/MMP-3 cd protein complex, permeability was decreased, and TJs were protected, as identified by decreasing permeability value to around 2.5-fold over vehicle-treated RBMECs (Fig. 5a).

MMP-9 showed a similar effect in increasing the permeability of RBMEC by disruption the TJs in a dose-dependent manner, although lower than MMP-3 cd, to a nearly 2.5-fold increase over baseline at 1.5 μM of MMP-9 cd consistent with other observation for MMP-9 degradation of BBB in previous studies [46-49]. In the presence of 1.5 μM of both TIMP-1 and MMP-9 cd, permeability was slightly over 1.5-fold over baseline (Fig. 5b), indicating partial inhibition the detrimental effect of TJ disruption. Studies have indicated that TIMP-1 treatment reduced BBB permeability that was disrupted by MMPs [50, 51]. According to our findings, the disruption of BBB was dependent of dosage of MMP-3 cd and MMP-9 cd, whereas administering TIMP-1 led to protection of BBB by inhibiting MMP-3 cd or MMP-9 cd (Fig. 5).

Effects of MMPs and TIMPs on TEER of RBMECs

The effect of MMP-3 or MMP-9 disruption of TJ, or TIMP-1 restoration of TJ integrity was evaluated by measuring TEER values on a monolayer of RBMEC after forming the BBB using an EVOM3 volt/ohm meter equipped. TEER resistance measurements are inversely correlated with membrane permeability. Significantly lower TEER values were observed when treated with MMP-3 cd and MMP-9 cd, and higher values measurements when MMPs were preincubated with TIMP-1 (Fig. 6). These results indicates that MMPs decreased the TEER values and TIMPs provided some protection from MMP-mediated drop in TEER measurements. Consistent with previous studies, the high TEER values indicate strong TJs and low permeability, while low TEER values indicate weak TJs and high permeability [52, 53], our results confirmed the formation of TJs in RBMECs and disruption of TJs by MMPs and protection by TIMP-1.

TJ formation in RBMECs and MMP-mediated disruption and TIMP-mediated protection of TJs

To investigate the presence of TJs within RBMECs, immunofluorescent staining of RBMEC with an antibody to the TJ protein ZO-1 was used. ZO-1 is one of the most abundant intracellular proteins found in TJs, and it plays a crucial role in the assembly of functional TJs by binding to a variety of TJ proteins and linking them to the actin cytoskeleton. It is regarded as essential for the assembly of TJs, and it also plays a critical role in maintaining the integrity and permeability of the BBB [54, 55]. TJ proteins, such as ZO-1, form a physical barrier between adjacent endothelial cells in the BBB and regulate the movement of molecules across this barrier. This fact is supported by numerous scientific studies and research articles in the field of neuroscience and physiology [56] that discuss the critical role of tight junction proteins in regulating BBB permeability and maintaining brain homeostasis or [57] that provide a comprehensive overview of the molecular mechanisms underlying BBB function, with a particular emphasis on the role of TJ proteins such as ZO-1. RBMEC have been shown to express TJ protein ZO-1 in monocultures [58-60].

After RBMEC reached 90% confluency on fibronectin-coated 35 mm glass base dishes, cells treated with 1.5 μM MMP-3 cd and/or 1.5 μM MMP-3 cd/TIMP-1 proteins for 1 h before fixation., the cells were checked under an inverted bright field microscope at 10X magnification (Fig. 7a). Immunofluorescent staining of TJ proteins was then performed after fixing and blocking the RBMEC and incubation with a primary polyclonal rabbit antibody against ZO-1, and secondary Alexa Fluor-488 by confocal microscopy (Fig. 7b). Our results illustrate that ZO-1 was clearly stained in the cell margins, indicating well-organized TJ that is characteristic of the BBB (Fig. 7b). In cells treated with 1.5 μM of MMP-3 cd for 1 h at 37°C, a lack of and rearrangement of ZO-1 staining was observed (Fig. 7b). Pretreatment with a TIMP-1 attenuated MMP-3 cd-induced disruption and reorganization of ZO-1 proteins and maintained baseline TJ integrity (Fig. 7b). These results confirmed the formation of TJs in RBMEC, disruption of TJs with MMP-3 cd, and protection of TJs from disruption using TIMP-1.

Conclusions

Disruption of the BBB occurs in neurological disorders, stroke, and other brain abnormalities, such as glioblastoma multiforme. BBB is known for its restrictive interface formed by brain microvascular endothelial cells (BMECs) that prevent most drugs from penetrating the brain. To evaluate the effect of MMP-mediated TJ degradation/BBB disruption and TIMP protection of BBB, an *in vitro* model of the BBB with rat BMECs were used [61, 62]. The unique TJs between neighboring BMECs are one of their characteristic properties, which makes them an ideal choice for studying the BBB [56, 63, 64]. BBB permeability of RBMECs has been extensively studied in the context of the BBB [32, 65-67]. To evaluate BBB permeability in RBMEC, we used various *in vitro* techniques such as permeability, TEER measurements, and ICC.

Our results indicated that the permeability of RBMEC can be modulated by the activity of MMPs and their inhibitors, TIMPs. MMPs protein disrupts the tight junctions of RBMEC in a dose-dependent manner and TIMP-1 protected tight junctions against MMP degradation. Based on our results, using the 1.5 μM of MMP-3 cd and TIMP-1 shows highest effect (Supplemental Fig. S1). Also, our results confirmed that the MMP-3 has more effect on the permeability of RBMEC by degrading TJ proteins compared to MMP-9, but TIMP-1's protective effect was greater for MMP-3 than MMP-9. We conclude that the MMPs can increase the permeability of RBMEC by degrading TJ proteins, leading to compromised BBB function. On the other hand, TIMPs can protect RBMEC by inhibiting MMP activity and preserving the integrity of TJs. Therefore, the balance between MMPs and TIMPs is critical for maintaining the BBB integrity and a healthy central nervous system. The *in vitro* BBB model mimics many key features of the *in vivo* BBB, such as TJs and transporters, and provide a more controlled setting for studying the effects of specific molecules and can be used for future experiments to evaluate effect and delivery of potential therapeutics across BBB. These therapeutics could be modified to carry cell penetrating peptides which facilitates transport across BBB [68]. The findings of this study contribute to the growing body of knowledge about the complex interactions between MMPs, TIMPs, and TJs in the BBB and highlight the potential of targeting these pathways for the treatment of neurological diseases that involve BBB dysfunction.

Supplementary Material

Refer to Web version on PubMed Central for supplementary material.

Acknowledgements

The authors acknowledge the UNR genomic center. The authors would also like to thank Dr. Robert Rendon for his help with confocal fluorescence microscopy and Dr. Eric Shusta for his scientific consultation on fluorescence microscopy *in vitro* BBB model.

Funding

M. R.-S. had funding support from NIH R03AG070511 and NIH R21HD109743.

Data Availability

The authors declare that the data supporting the findings of this study are available within the paper and its Supplementary Information files. Should any raw data files be needed in another format they are available from the corresponding author upon reasonable request.

References

1. Yong VW, Power C, Forsyth P, Edwards DR. Metalloproteinases in biology and pathology of the nervous system. Nat Rev Neurosci. 2001;2(7):502–11. 10.1038/35081571. [PubMed: 11433375]
2. Cunningham LA, Wetzel M, Rosenberg GA. Multiple roles for MMPs and TIMPs in cerebral ischemia. Glia. 2005;50(4):329–39. 10.1002/glia.20169. [PubMed: 15846802]
3. Raeeszadeh-Sarmazdeh M, Do LD, Hritz BG. Metalloproteinases and Their Inhibitors: Potential for the Development of New Therapeutics. Cells. 2020;9(5). 10.3390/cells9051313.
4. Asahi M, Wang X, Mori T, Sumii T, Jung JC, Moskowitz MA, et al. Effects of matrix metalloproteinase-9 gene knock-out on the proteolysis of blood-brain barrier and white matter components after cerebral ischemia. J Neurosci. 2001;21(19):7724–32. 10.1523/JNEUROSCI.21-19-07724.2001. [PubMed: 11567062]
5. Harkness KA, Adamson P, Sussman JD, Davies-Jones GA, Greenwood J, Woodroofe MN. Dexamethasone regulation of matrix metalloproteinase expression in CNS vascular endothelium. Brain. 2000;123(Pt 4):698–709. 10.1093/brain/123.4.698. [PubMed: 10734001]
6. Fukuda S, Fini CA, Mabuchi T, Koziol JA, Eggleston LL, del Zoppo GJ. Focal cerebral ischemia induces active proteases that degrade microvascular matrix. Stroke. 2004;35(4):998–1004. 10.1161/01.STR.0000119383.76447.05. [PubMed: 15001799]
7. Hamann GF, Okada Y, Fitridge R, del Zoppo GJ. Microvascular basal lamina antigens disappear during cerebral ischemia and reperfusion. Stroke. 1995;26(11):2120–6. 10.1161/01.str.26.11.2120. [PubMed: 7482660]
8. Song LQ, Oseid DE, Wells EA, Coaston T, Robinson AS. Heparan Sulfate Proteoglycans (HSPGs) Serve as the Mediator Between Monomeric Tau and Its Subsequent Intracellular ERK1/2 Pathway Activation. J Mol Neurosci. 2022;72(4):772–91. 10.1007/s12031-021-01943-2. [PubMed: 35040015]
9. Gurney KJ, Estrada EY, Rosenberg GA. Blood-brain barrier disruption by stromelysin-1 facilitates neutrophil infiltration in neuroinflammation. Neurobiol Dis. 2006;23(1):87–96. 10.1016/j.nbd.2006.02.006. [PubMed: 16624562]
10. Banks WA. Characteristics of compounds that cross the blood-brain barrier. BMC Neurol. 2009;9 Suppl 1(Suppl 1):3. 10.1186/1471-2377-9-S1-S3. [PubMed: 19144113]
11. Banks WA, Greig NH. Small molecules as central nervous system therapeutics: old challenges, new directions, and a philosophic divide. Future Med Chem. 2019;11(6):489–93. 10.4155/fmc-2018-0436. [PubMed: 30912980]
12. Reese TS, Karnovsky MJ. Fine structural localization of a blood-brain barrier to exogenous peroxidase. J Cell Biol. 1967;34(1):207–17. 10.1083/jcb.34.1.207. [PubMed: 6033532]
13. Iwatake A, Murakami A, Ebihara N. The expression of matrix metalloproteinases and their inhibitors in corneal fibroblasts by alarmins from necrotic corneal epithelial cells. Jpn J Ophthalmol. 2018;62(1):92–100. 10.1007/s10384-017-0541-x. [PubMed: 29094325]
14. Van Hove I, Lemmens K, Van de Velde S, Verslegers M, Moons L. Matrix metalloproteinase-3 in the central nervous system: a look on the bright side. J Neurochem. 2012;123(2):203–16. 10.1111/j.1471-4159.2012.07900.x. [PubMed: 22862420]
15. Rosenberg GA. Matrix metalloproteinases and their multiple roles in neurodegenerative diseases. Lancet Neurol. 2009;8(2):205–16. 10.1016/S1474-4422(09)70016-X. [PubMed: 19161911]
16. Rosenberg GA, Yang Y. Vasogenic edema due to tight junction disruption by matrix metalloproteinases in cerebral ischemia. Neurosurg Focus. 2007;22(5):E4. 10.3171/foc.2007.22.5.5.

17. Wang X, Jung J, Asahi M, Chwang W, Russo L, Moskowitz MA, et al. Effects of matrix metalloproteinase-9 gene knock-out on morphological and motor outcomes after traumatic brain injury. J Neurosci. 2000;20(18):7037–42. 10.1523/JNEUROSCI.20-18-07037.2000. [PubMed: 10995849]

18. Becker JW, Marcy AI, Rokosz LL, Axel MG, Burbaum JJ, Fitzgerald PM, et al. Stromelysin-1: three-dimensional structure of the inhibited catalytic domain and of the C-truncated proenzyme. Protein Sci. 1995;4(10):1966–76. 10.1002/pro.5560041002. [PubMed: 8535233]

19. Nagase H, Woessner JF. Matrix metalloproteinases. J Biol Chem. 1999;274(31):21491–4. 10.1074/jbc.274.31.21491. [PubMed: 10419448]

20. Baker AH, Edwards DR, Murphy G. Metalloproteinase inhibitors: biological actions and therapeutic opportunities. J Cell Sci. 2002;115(Pt 19):3719–27. 10.1242/jcs.00063. [PubMed: 12235282]

21. Stetler-Stevenson WG. Matrix metalloproteinases in angiogenesis: a moving target for therapeutic intervention. J Clin Invest. 1999;103(9):1237–41. 10.1172/JCI6870. [PubMed: 10225966]

22. Dreymueller D, Pruessmeyer J, Groth E, Ludwig A. The role of ADAM-mediated shedding in vascular biology. Eur J Cell Biol. 2012;91(6–7):472–85. 10.1016/j.ejcb.2011.09.003. [PubMed: 22138087]

23. Dreymueller D, Martin C, Kogel T, Pruessmeyer J, Hess FM, Horiuchi K, et al. Lung endothelial ADAM17 regulates the acute inflammatory response to lipopolysaccharide. EMBO Mol Med. 2012;4(5):412–23. 10.1002/emmm.201200217. [PubMed: 22367719]

24. Brew K, Nagase H. The tissue inhibitors of metalloproteinases (TIMPs): an ancient family with structural and functional diversity. Biochim Biophys Acta. 2010;1803(1):55–71. 10.1016/j.bbamcr.2010.01.003. [PubMed: 20080133]

25. Masciantonio MG, Lee CKS, Arpino V, Mehta S, Gill SE. The Balance Between Metalloproteinases and TIMPs: Critical Regulator of Microvascular Endothelial Cell Function in Health and Disease. Prog Mol Biol Transl Sci. 2017;147:101–31. 10.1016/bs.pmbts.2017.01.001. [PubMed: 28413026]

26. Murphy G. Tissue inhibitors of metalloproteinases. Genome Biol. 2011;12(11):233. 10.1186/gb-2011-12-11-233. [PubMed: 22078297]

27. Yang Y, Estrada EY, Thompson JF, Liu W, Rosenberg GA. Matrix metalloproteinase-mediated disruption of tight junction proteins in cerebral vessels is reversed by synthetic matrix metalloproteinase inhibitor in focal ischemia in rat. J Cereb Blood Flow Metab. 2007;27(4):697–709. 10.1038/sj.jcbfm.9600375. [PubMed: 16850029]

28. Fujimoto M, Takagi Y, Aoki T, Hayase M, Marumo T, Gomi M, et al. Tissue inhibitor of metalloproteinases protect blood-brain barrier disruption in focal cerebral ischemia. J Cereb Blood Flow Metab. 2008;28(10):1674–85. 10.1038/jcbfm.2008.59. [PubMed: 18560439]

29. Deli MA, Abrahám CS, Kataoka Y, Niwa M. Permeability studies on in vitro blood-brain barrier models: physiology, pathology, and pharmacology. Cell Mol Neurobiol. 2005;25(1):59–127. 10.1007/s10571-004-1377-8. [PubMed: 15962509]

30. Abbott NJ, Dolman DE, Drndarski S, Fredriksson SM. An improved in vitro blood-brain barrier model: rat brain endothelial cells co-cultured with astrocytes. Methods Mol Biol. 2012;814:415–30. 10.1007/978-1-61779-452-0_28. [PubMed: 22144323]

31. Srinivasan B, Kolli AR, Esch MB, Abaci HE, Shuler ML, Hickman JJ. TEER measurement techniques for in vitro barrier model systems. J Lab Autom. 2015;20(2):107–26. 10.1177/2211068214561025. [PubMed: 25586998]

32. Helms HC, Abbott NJ, Burek M, Cecchelli R, Couraud PO, Deli MA, et al. In vitro models of the blood-brain barrier: An overview of commonly used brain endothelial cell culture models and guidelines for their use. J Cereb Blood Flow Metab. 2016;36(5):862–90. 10.1177/0271678X16630991. [PubMed: 26868179]

33. Geldenhuys WJ, Mohammad AS, Adkins CE, Lockman PR. Molecular determinants of blood-brain barrier permeation. Ther Deliv. 2015;6(8):961–71. 10.4155/tde.15.32. [PubMed: 26305616]

34. Daneman R, Prat A. The blood-brain barrier. Cold Spring Harb Perspect Biol. 2015;7(1):a020412. 10.1101/cshperspect.a020412. [PubMed: 25561720]

35. Raeeszadeh-Sarmazdeh M, Coban M, Mahajan S, Hockla A, Sankaran B, Downey GP, et al. Engineering of tissue inhibitor of metalloproteinases TIMP-1 for fine discrimination between closely related stromelysins MMP-3 and MMP-10. J Biol Chem. 2022;298(3):101654. 10.1016/j.jbc.2022.101654. [PubMed: 35101440]
36. Bolt AJ, Do LD, Raeeszadeh-Sarmazdeh M. Bacterial Expression and Purification of Human Matrix Metalloproteinase-3 using Affinity Chromatography. J Vis Exp. 2022(181). 10.3791/63263
37. Raeeszadeh-Sarmazdeh M, Greene KA, Sankaran B, Downey GP, Radisky DC, Radisky ES. Directed evolution of the metalloproteinase inhibitor TIMP-1 reveals that its N- and C-terminal domains cooperate in matrix metalloproteinase recognition. J Biol Chem. 2019;294(24):9476–88. 10.1074/jbc.RA119.008321. [PubMed: 31040180]
38. Toumaian MR, Raeeszadeh-Sarmazdeh M. Engineering Tissue Inhibitors of Metalloproteinases Using Yeast Surface Display. Methods Mol Biol. 2022;2491:361–85. 10.1007/978-1-0716-2285-8_19. [PubMed: 35482200]
39. Liu J, Jin X, Liu KJ, Liu W. Matrix metalloproteinase-2-mediated occludin degradation and caveolin-1-mediated claudin-5 redistribution contribute to blood-brain barrier damage in early ischemic stroke stage. J Neurosci. 2012;32(9):3044–57. 10.1523/JNEUROSCI.6409-11.2012. [PubMed: 22378877]
40. Jones AR, Shusta EV. Blood-brain barrier transport of therapeutics via receptor-mediation. Pharm Res. 2007;24(9):1759–71. 10.1007/s11095-007-9379-0. [PubMed: 17619996]
41. Gumbleton M, Audus KL. Progress and limitations in the use of in vitro cell cultures to serve as a permeability screen for the blood-brain barrier. J Pharm Sci. 2001;90(11):1681–98. 10.1002/jps.1119. [PubMed: 11745727]
42. Reichel A, Begley DJ, Abbott NJ. An overview of in vitro techniques for blood-brain barrier studies. Methods Mol Med. 2003;89:307–24. 10.1385/1-59259-419-0:307. [PubMed: 12958429]
43. Gaillard PJ, de Boer AG. Relationship between permeability status of the blood-brain barrier and in vitro permeability coefficient of a drug. Eur J Pharm Sci. 2000;12(2):95–102. 10.1016/s0928-0987(00)00152-4. [PubMed: 11102736]
44. Zhang Q, Zheng M, Betancourt CE, Liu L, Sitikov A, Sladojevic N, et al. Increase in Blood-Brain Barrier (BBB) Permeability Is Regulated by MMP3 via the ERK Signaling Pathway. Oxid Med Cell Longev. 2021;2021:6655122. 10.1155/2021/6655122. [PubMed: 33859779]
45. Gomis-Ruth FX, Maskos K, Betz M, Bergner A, Huber R, Suzuki K, et al. Mechanism of inhibition of the human matrix metalloproteinase stromelysin-1 by TIMP-1. Nature. 1997;389(6646):77–81. 10.1038/37995. [PubMed: 9288970]
46. Brilha S, Ong CWM, Weksler B, Romero N, Couraud PO, Friedland JS. Matrix metalloproteinase-9 activity and a downregulated Hedgehog pathway impair blood-brain barrier function in an in vitro model of CNS tuberculosis. Sci Rep. 2017;7(1):16031. 10.1038/s41598-017-16250-3. [PubMed: 29167512]
47. Nguyen JH, Yamamoto S, Steers J, Sevlever D, Lin W, Shimojima N, et al. Matrix metalloproteinase-9 contributes to brain extravasation and edema in fulminant hepatic failure mice. J Hepatol. 2006;44(6):1105–14. 10.1016/j.jhep.2005.09.019. [PubMed: 16458990]
48. Salah MM, Abdelmawla MA, Eid SR, Hasanin RM, Mostafa EA, Abdelhameed MW. Role of Matrix Metalloproteinase-9 in Neonatal Hypoxic-Ischemic Encephalopathy. Open Access Maced J Med Sci. 2019;7(13):2114–8. 10.3889/oamjms.2019.618. [PubMed: 31456835]
49. Liu X, Su P, Meng S, Aschner M, Cao Y, Luo W, et al. Role of matrix metalloproteinase-2/9 (MMP2/9) in lead-induced changes in an. Int J Biol Sci. 2017;13(11):1351–60. 10.7150/ijbs.20670. [PubMed: 29209140]
50. Tang J, Kang Y, Huang L, Wu L, Peng Y. TIMP1 preserves the blood-brain barrier through interacting with CD63/integrin. Acta Pharm Sin B. 2020;10(6):987–1003. 10.1016/j.apsb.2020.02.015. [PubMed: 32642407]
51. Lakhan SE, Kirchgessner A, Tepper D, Leonard A. Matrix metalloproteinases and blood-brain barrier disruption in acute ischemic stroke. Front Neurol. 2013;4:32. 10.3389/fneur.2013.00032. [PubMed: 23565108]
52. Hyatt AD, Eaton BT. Virological applications of the grid-cell-culture technique. Electron Microsc Rev. 1990;3(1):1–27. 10.1016/0892-0354(90)90011-g. [PubMed: 1966471]

53. Huber JD, Egleton RD, Davis TP. Molecular physiology and pathophysiology of tight junctions in the blood-brain barrier. Trends Neurosci. 2001;24(12):719–25. 10.1016/s0166-2236(00)02004-x. [PubMed: 11718877]
54. Prime SS, Nixon SV, Crane IJ, Stone A, Matthews JB, Maitland NJ, et al. The behaviour of human oral squamous cell carcinoma in cell culture. J Pathol. 1990;160(3):259–69. 10.1002/path.1711600313. [PubMed: 1692339]
55. Shin K, Margolis B. ZOning out tight junctions. Cell. 2006;126(4):647–9. 10.1016/jxell.2006.08.005. [PubMed: 16923383]
56. Hawkins BT, Davis TP. The blood-brain barrier/neurovascular unit in health and disease. Pharmacol Rev. 2005;57(2):173–85. 10.1124/pr.57.2.4. [PubMed: 15914466]
57. Obermeier B, Daneman R, Ransohoff RM. Development, maintenance and disruption of the blood-brain barrier. Nat Med. 2013;19(12):1584–96. 10.1038/nm.3407. [PubMed: 24309662]
58. Nakagawa S, Deli MA, Kawaguchi H, Shimizudani T, Shimono T, Kittel A, et al. A new blood-brain barrier model using primary rat brain endothelial cells, pericytes and astrocytes. Neurochem Int. 2009;54(3–4):253–63. 10.1016/j.neuint.2008.12.002. [PubMed: 19111869]
59. Calabria AR, Weidenfeller C, Jones AR, de Vries HE, Shusta EV. Puromycin-purified rat brain microvascular endothelial cell cultures exhibit improved barrier properties in response to glucocorticoid induction. J Neurochem. 2006;97(4):922–33. 10.1111/j.1471-4159.2006.03793.x. [PubMed: 16573646]
60. Cardoso FL, Kittel A, Veszelka S, Palmela I, Tóth A, Brites D, et al. Exposure to lipopolysaccharide and/or unconjugated bilirubin impair the integrity and function of brain microvascular endothelial cells. PLoS One. 2012;7(5):e35919. 10.1371/journal.pone.0035919. [PubMed: 22586454]
61. Veszelka S, Tóth A, Walter FR, Tóth AE, Gróf I, Mészáros M, et al. Comparison of a Rat Primary Cell-Based Blood-Brain Barrier Model With Epithelial and Brain Endothelial Cell Lines: Gene Expression and Drug Transport. Front Mol Neurosci. 2018;11:166. 10.3389/fnmol.2018.00166. [PubMed: 29872378]
62. Aday S, Cecchelli R, Hallier-Vanuxeem D, Dehouck MP, Ferreira L. Stem Cell-Based Human Blood-Brain Barrier Models for Drug Discovery and Delivery. Trends Biotechnol. 2016;34(5):382–93. 10.1016/j.tibtech.2016.01.001. [PubMed: 26838094]
63. Abbott NJ, Patabendige AA, Dolman DE, Yusof SR, Begley DJ. Structure and function of the blood-brain barrier. Neurobiol Dis. 2010;37(1):13–25. 10.1016/j.nbd.2009.07.030. [PubMed: 19664713]
64. Zlokovic BV. The blood-brain barrier in health and chronic neurodegenerative disorders. Neuron. 2008;57(2):178–201. 10.1016/j.neuron.2008.01.003. [PubMed: 18215617]
65. Molino Y, Jabès F, Lacassagne E, Gaudin N, Khrestchatisky M. Setting-up an in vitro model of rat blood-brain barrier (BBB): a focus on BBB impermeability and receptor-mediated transport. J Vis Exp. 2014;88:51278. 10.3791/51278.
66. Díaz-Coránguez M, Segovia J, López-Ornelas A, Puerta-Guardo H, Ludert J, Chávez B, et al. Transmigration of neural stem cells across the blood brain barrier induced by glioma cells. PLoS One. 2013;8(4):e60655. 10.1371/journal.pone.0060655. [PubMed: 23637756]
67. Yan XB, Zhao YF, Yang YM, Wang N, He BZ, Qiu XT. Impact of astrocyte and lymphocyte interactions on the blood-brain barrier in multiple sclerosis. Rev Neurol (Paris). 2019;175(6):396–402. 10.1016/j.neurol.2018.12.006. [PubMed: 31027862]
68. Safa N, Pettigrew JH, Gauthier TJ, Melvin AT. Direct measurement of deubiquitinating enzyme activity in intact cells using a protease-resistant, cell-permeable, peptide-based reporter. Biochem Eng J. 2019;151:ARTN 107320. 10.1016/j.bej.2019.107320. [PubMed: 32831622]

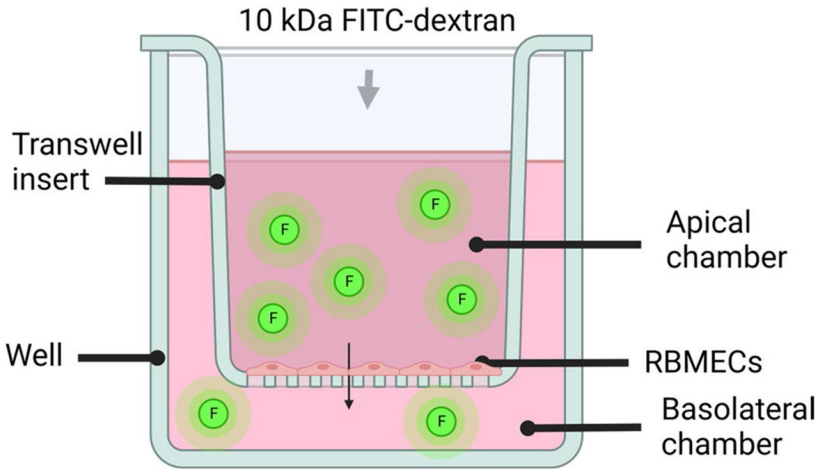

Fig. 1.

A schematic of the blood-brain barrier model. The simplified *in vitro* blood brain barrier (BBB) model uses rat brain endothelial cell (RBMEC). RBMECs were grown on the Transwell® inserts to form a confluent monolayer. The permeability was measured after adding FITC-conjugated dextran (MW: 10 kDa) to the apical chamber while samples were taken from the basolateral chamber at 30- or 15-min time intervals for 2 h.

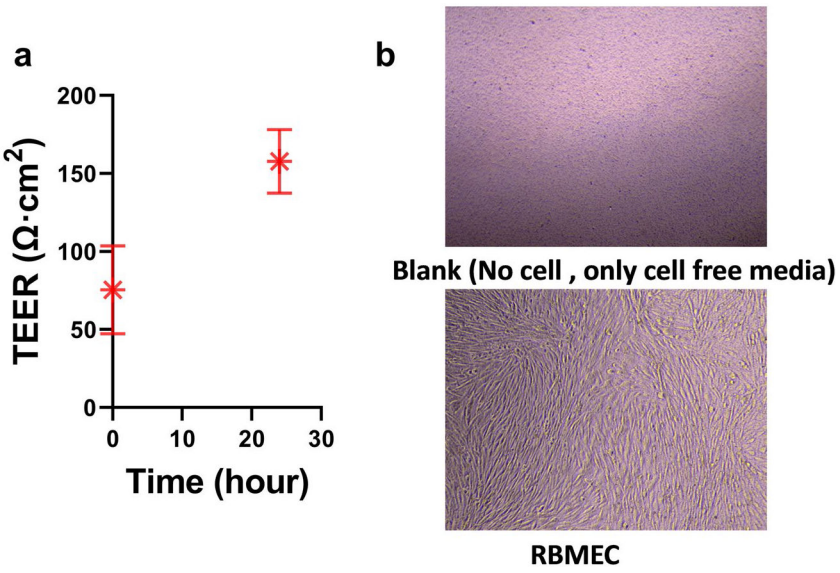

Fig. 2.

Confirming the RBMEC growth by TEER and microscopy. (**a**) The TEER value was measured immediately after transferring the cells (n = 17) into 24-well Transwells (time = 0) and after 24 h. (**b**) The bright field microscopy images (Fisherbrand™ Entry Level Research Grade Inverted Microscope, Fisher Scientific, USA, at 10X magnification) of RBMEC on Transwells, are shown after 24 h incubation at 37°C incubator when the TEER value exceeded 150 Ω × cm^2. The top image is blank (no cells, collagen/fibronectin-coated Transwell only) and the bottom is the RBMECs grown after 24 h incubation.

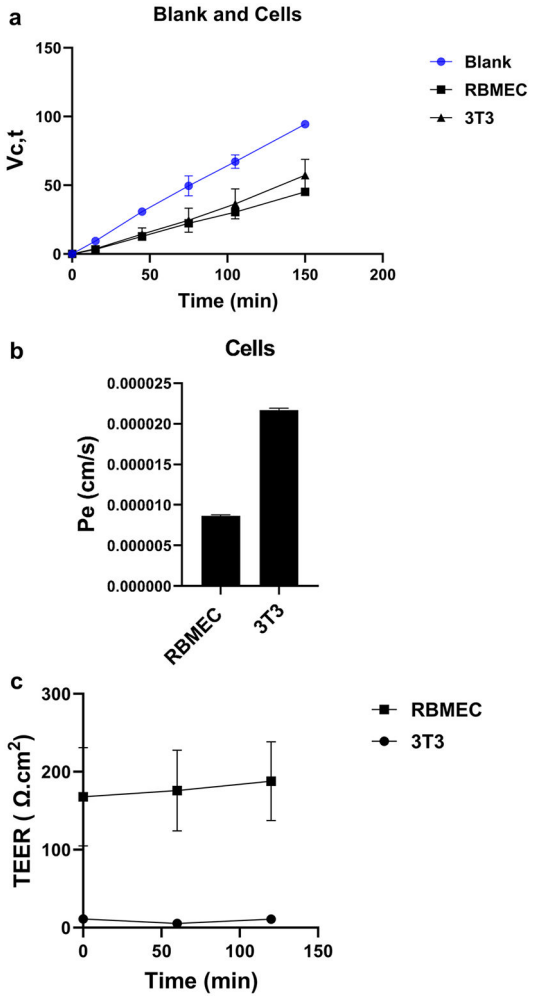

Fig. 3.

The permeability level of RBMEC and 3T3 cells was compared over time. (**a**) Comparison between blank (no cells, collagen/fibronectin-coated Transwell only), RBMEC, and 3T3 cells. Time points were taken every 30 min. (**b**) Permeability value for 3T3 cells *vs.* RBMEC, (**c**) The RBMEC TEER value exceeded 150 Ω × cm^2 but the TEER value of 3T3 cells was less than 10 Ω × cm^2. Experiment was performed in duplicate with the 12-well Transwell ($V_{C,t}$ = 1500 μl × $S_{b,t}$ / S_a).

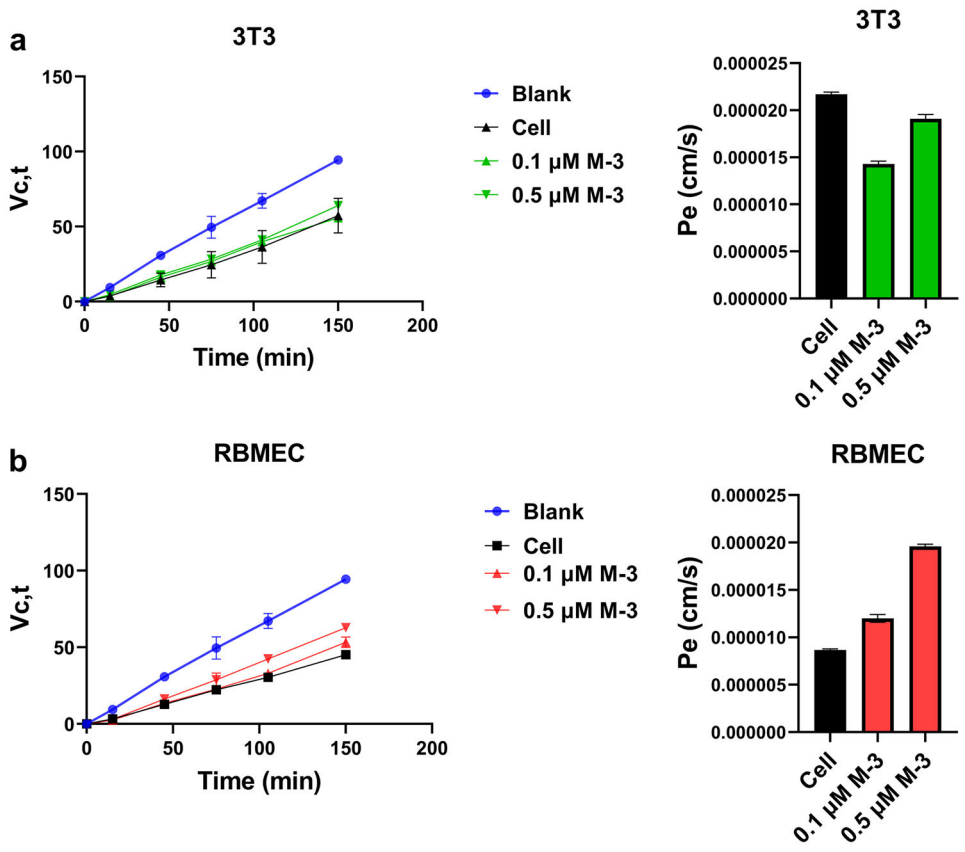

Fig. 4.

The permeability of RBMEC and 3T3 cells after treating with different concentration of MMP-3 cd was compared in time dependence manner. (**a**) Time point value (left) and Pe value bar graphs (right) for permeability of 3T3 cells before and after MMP-3 cd (M-3) treatment, (**b**) Time point value (left) and Pe value bar graphs (right) for permeability RBMEC before and after MMP-3 cd (M-3) treatment. Experiment was performed with 12-well Transwells ($V_{C,t}$ = 1500 μl × $S_{b,t}$ / S_a) and repeated at least three times. The error bars represent standard deviation.

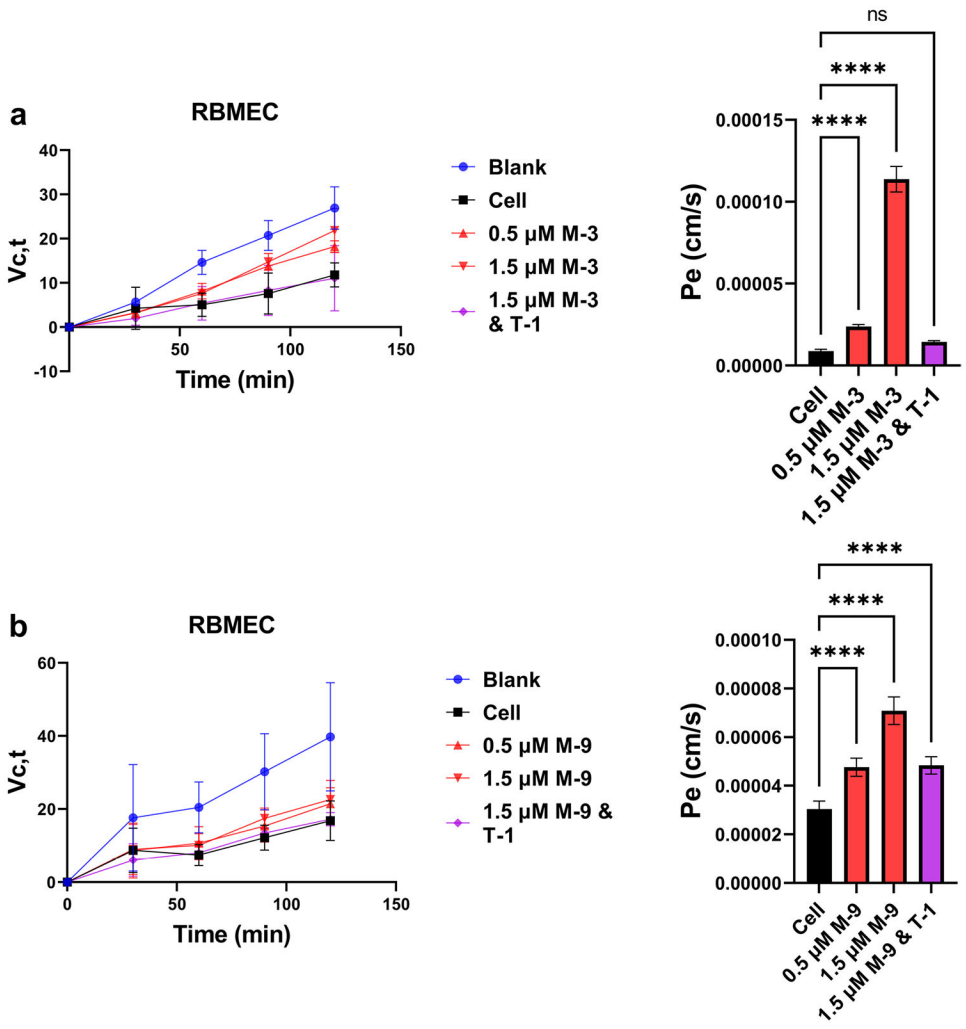

Fig. 5.

Effect of MMP-3 cd and MMP-9 cd and their complex with TIMP-1 on permeability of RBMEC. (**a**) MMP-3 cd disrupts the tight junctions of RBMECs in a dose-dependent manner based on 5 replicate experiments from 3 different groups of RBMEC leading to a nearly 18-fold increase over baseline permeability at 1.5 μM of MMP-3 cd. In the presence of 1.5 μM of both TIMP-1 and MMP-3 cd, permeability was slightly over two and half of baseline (p-value: **** < 0.0001). Experiment was performed in 24-well Transwells ($V_{c,t}$ = 600 μl × $S_{b,t}$ / S_a). (**b**) MMP-9 cd disrupts the tight junctions of RBMEC in a dose-dependent manner based on an average of 5 different wells from 3 different groups of RBMEC leading to a nearly 2.5-fold increase over baseline permeability at 1.5 μM of MMP-9 cd. In the presence of 1.5 μM of both TIMP-1 and MMP-9 cd, permeability was slightly over one and half of baseline (p-value: **** < 0.0001). (M-3: MMP-3 cd, M-9: MMP-9 cd, T-1: TIMP-1). Experiment was performed in 24-well Transwells ($V_{c,t}$ = 600 μl × $S_{b,t}$ / S_a).

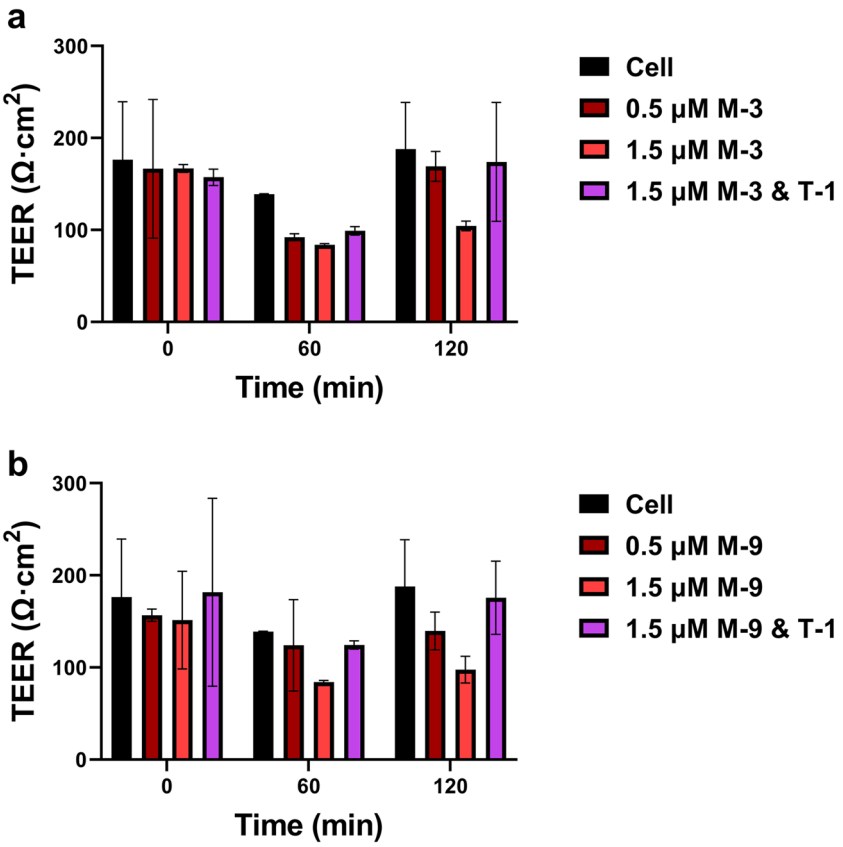

Fig. 6.

TEER of MMP-3 cd and MMP-9 cd alone or with TIMP-1 on RBMEC. (**a**) The TEER value of RBMEC after treating with MMP-3 cd alone or with MMP-3 cd in complex with TIMP-1, and (**b**) with MMP-9 cd alone or in complex with TIMP-1 was compared at 60-min intervals for 2 h. (M-3: MMP-3 cd, M-9: MMP-9 cd, T1: TIMP-1). Each experiment repeated three times, and the error bar shows the standard deviation.

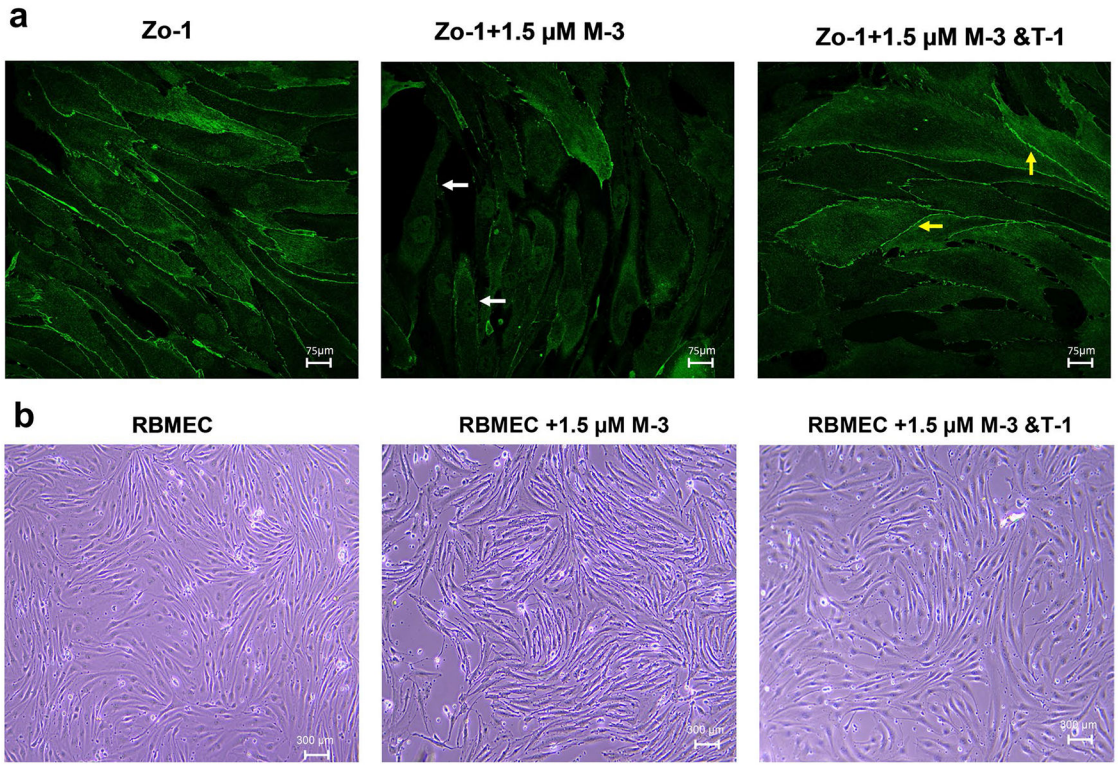

Fig. 7.

Confirming the effect of MMP-3 cd alone or with TIMP-1 on RBMEC by ICC. (**a**) RBMEC on 35 glass base dishes without treatment, after 1 h treatment with 1.5 μM MMP-3 cd and after 1 h treatment with preincubated 1.5 μM MMP-3 cd and 1.5 μM TIMP-1 by inverted bright field microscope at 10X magnification (**b**) ICC image of RBMEC, as primary antibody 1/50 Zo-1 used and as secondary antibody AlexaFluor 488 (rabbit) used by confocal fluorescent microscope at 60X magnification (M-3: MMP-3 cd, T-1: TIMP-1). The arrows highlight some of the observations for disruption (white, MMP-3 treated), or protection (yellow, TIMP-1 in complex with MMP-3 treated).